BBA - Molecular and Cell Biology of Lipids 1863 (2018) 980–990

Contents lists available at ScienceDirect

BBA - Molecular and Cell Biology of Lipids

journal homepage: www.elsevier.com/locate/bbalip

High-fat diet-induced lipidome perturbations in the cortex, hippocampus, hypothalamus, and olfactory bulb of mice

Jong Cheol Lee[a], Se Mi Park[a], Il Yong Kim[b,c], Hyerim Sung[b,c], Je Kyung Seong[b,c,d,**], Myeong Hee Moon[a,*]

[a] Department of Chemistry, Yonsei University, Seoul 03722, Republic of Korea
[b] Laboratory of Developmental Biology and Genomics, BK21 Program Plus for Advanced Veterinary Science, Research Institute for Veterinary Science, College of Veterinary Medicine, Seoul National University, Seoul, Republic of Korea
[c] Korea Mouse Phenotyping Center (KMPC), Seoul, Republic of Korea
[d] Interdisciplinary Program for Bioinformatics, Program for Cancer Biology and BIO-MAX/N-Bio Institute, Seoul National University, Seoul, Republic of Korea

ARTICLE INFO

Keywords:
High-fat diet
Brain lipidome
Mouse
nUPLC-ESI-MS/MS

ABSTRACT

Given their important role in neuronal function, there has been an increasing focus on altered lipid levels in brain disorders. The effect of a high-fat (HF) diet on the lipid profiles of the cortex, hippocampus, hypothalamus, and olfactory bulb of the mouse brain was investigated using nanoflow ultrahigh pressure liquid chromatography-electrospray ionization-tandem mass spectrometry in the current study. For 8 weeks, two groups of 5-week-old mice were fed either an HF or normal diet (6 mice from each group analyzed as the F and N groups, respectively). The remaining mice in both groups then received a 4-week normal diet. Each group was then subdivided into two groups for another 4-week HF or normal diet. Quantitative analysis of 270 of the 359 lipids identified from brain tissue revealed that an HF diet significantly affected the brain lipidome in all brain regions that were analyzed. The HF diet significantly increased diacylglycerols, which play a role in insulin resistance in all regions that were analyzed. Although the HF diet increased most lipid species, the majority of phosphatidylserine species were decreased, while lysophosphatidylserine species, with the same acyl chain, were substantially increased. This result can be attributed to increased oxidative stress due to the HF diet. Further, weight-cycling (yo-yo effect) was found more critical for the perturbation of brain lipid profiles than weight gain without a preliminary experience of an HF diet. The present study reveals systematic alterations in brain lipid levels upon HF diet analyzed either by lipid class and molecular levels.

1. Introduction

Lipids play an essential role, not only in energy storage and the formation of cellular membrane structures, but also in cell signaling, proliferation, and apoptosis [1,2]. Recent studies demonstrated that lipid profile perturbations are related to the pathogenesis of metabolic diseases like obesity, diabetes, coronary artery diseases, cancers, and rare diseases [3–6]. Moreover, lipids play an important role in neuronal (nerve cells) function in the brain [7]. Thus, lipidomic analysis in relation to brain disorders has gained attention.

The brain is one of the most complex organs belonging to the central nervous system and is involved with perception, learning and memory, motion, and metabolic activities, which result from the communication between neurons in the brain, via a combination of electrical and chemical signals [8,9]. Due its important role, brain dysfunction may cause serious illness that deteriorates the quality of life. Recently, alterations in lipid levels in the brain have been reported as risk factors for neurodegenerative disorders, such as Alzheimer's disease, Huntington's disease, and Parkinson's disease [10–12]. Several studies demonstrated decreased levels of sphingomyelins (SMs) and

Abbreviations: BEH, ethylene bridged hybrid; Cer, ceramide; DHA, docosahexaenoic acid; FA, fatty acid; HF, high-fat; IPA, isopropanol; IS, internal standard; LPA, lysophosphatidic acid; LPC, lysophosphatidylcholine; LPE, lysophosphatidylethanolamine; LPG, lysophosphatidylglycerol; LPI, lysophosphatidylinositol; LPS, lysophosphatidylserine; MHC, monohexosylceramide; MTBE, methyl-*tert*-butyl ether; nUPLC-ESI-MS/MS, nanoflow ultrahigh pressure liquid chromatography-electrospray ionization-tandem mass spectrometry; PA, phosphatidic acid; PC, phosphatidylcholine; PCA, principal component analysis; PE, phosphatidylethanolamine; PEp, PE plasmalogen; PG, phosphatidylglycerol; PI, phosphatidylinositol; PL, phospholipids; PS, phosphatidylserine; PUFA, polyunsaturated fatty acid; SM, sphingomyelin; SRM, selected reaction monitoring; ST, sulfatide; DAG, diacylglycerol; TAG, triacylglycerol

* Correspondence to: M.H. Moon, Department of Chemistry, Yonsei University, Seoul 03722, Republic of Korea.
** Corresponding author.
E-mail addresses: snumouse@snu.ac.kr (J.K. Seong), mhmoon@yonsei.ac.kr (M.H. Moon).

https://doi.org/10.1016/j.bbalip.2018.05.007
Received 24 November 2017; Received in revised form 12 April 2018; Accepted 14 May 2018
Available online 19 May 2018
1388-1981/

polyunsaturated fatty acid (PUFA), and increased levels of ceramides and oxidative products, including unsaturated aldehydes, as a result of enhanced lipid peroxidation in Alzheimer's disease [13–16]. There is also evidence that the lipid composition of the brain may influence perception and emotional behavior, which may lead to depression and anxiety disorders [12,17,18]. Lipidomic analysis revealed highly abundant plasma levels of phosphatidylcholine (PC) and triacylglycerol (TAG), in general, and a significant increase in TAGs containing two or three saturated fatty acyl chains, in particular, in patients with hypertension [19]. Studies suggest that the alterations in the composition of brain lipids can be caused by long-term changes in diet [17]. Further, animal studies demonstrated that a lack of n-3 PUFA in the brain can induce depression or anxiety related behavior [20,21]. Therefore, altered lipid metabolism in the brain may be a critical factor in central nervous system injuries and the effect of diet on lipidomic propagations in the brain is of importance to understanding brain disorders and its possible prevention with the help of healthy foods.

The food we eat contains lipids, particularly fats that include TAGs, cholesterol, and phospholipids (PLs) that contain fatty acids (FAs). Although saturated and monounsaturated FAs are synthesized within the brain, some PUFAs such as linoleic acid, α-linoleic acid, arachidonic acid, and docosahexaenoic acid (DHA) need to be supplied through the diet via the blood [22,23]. DHA plays a role in learning and memory and has been reported to promote neuronal survival and neurogenesis [24,25]. It may have preventive or therapeutic roles in Alzheimer's disease and depression [26,27]. A HF diet, however, is generally rich in saturated fats and is known to induce obesity, cognitive impairment, and neurodegenerative diseases [28]. Studies demonstrate that an HF diet can impair neurogenesis through lipid peroxidation and decrease brain-derived neurotropic factor [28], induce anxiety disorder [29], and is associated with the decrease in the volume of the hippocampus, which plays a role in learning, memory, and mood regulation [30]. Moreover, chronic consumption of an HF diet causes diet-induced obesity, resulting in insulin resistance in neurons of the hypothalamus, i.e., the main area controlling energy intake and consumption [31]. Although the effect of an HF diet on brain health has been studied in pathogenesis, the relationship between an HF diet and lipidomic changes in the brain has not been widely examined, except in a few studies on mice, which analyzed the effect of an HF diet on hypothalamic lipid accumulation [32] and on cerebral lipid species in comparison to plasma lipids [33].

Lipids are classified with the following categories: PLs, glycerolipids, sphingolipids, sterols, FAs, prenols, etc. Due to the complexity in their molecular structure, including differences in the polar head group, length of fatty acyl chain, degree of unsaturation, and substitutions with glycans, lipid analysis often requires a comprehensive analytical approach. Recently, liquid chromatography (LC) combined with electrospray ionization-tandem mass spectrometry (ESI-MS/MS), facilitated the simultaneous separation and structural determination of intact lipid molecules from plasma or urine samples of patients with various diseases, including colorectal cancer, breast cancer, and diabetes [34–37]. Incorporation of capillary LC at nanoflow regime empowered the capability of lipidomic analysis to be performed at low fmol levels [38,39], with high-speed targeted quantitation (< 20 min) of > 300 lipid molecules [40]. In our laboratory, it has been powerfully applied to study lipidomic alterations in plasma and urine of patients with Gaucher disease [6], skeletal muscles from diabetic rats after exercise [41], internal organs and brain tissues mice after p53 knockout [42,43], and urinary exosomes of patients with prostate cancer [44].

In the current study, the effect of an HF diet on the lipid profile of four different brain regions (i.e., the cortex, hippocampus, hypothalamus, and olfactory bulb) of mice were comprehensively examined at the molecular level. The present study not only profiled the mouse lipidome with an 8-week HF diet (F) or normal diet (N), but also examined systematic differences by varying the periods of the HF diet as shown in Fig. 1. The lipidomic analysis was first conducted with non-targeted identification of lipid molecular structures using nanoflow ultrahigh pressure LC-ESI-tandem MS (nUPLC-ESI-MS/MS), followed by high-speed targeted quantification of individual lipid samples using the selected reaction monitoring (SRM) method. From the statistical evaluation of quantified data, differences of lipid profiles among different brain tissues were investigated at the level of lipid classes. The effect of the HF diet on the lipidome were examined at both the lipid class and molecular levels, in the different brain regions, according to the different diet programs, including weight gain, weight maintenance, and weight cycling.

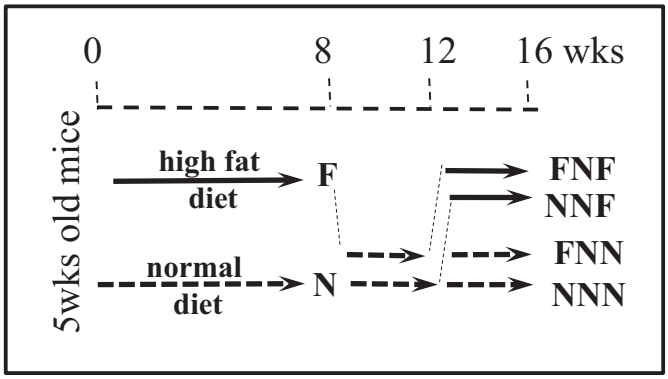

Fig. 1. A total of 6 different mouse groups were analyzed in this current study, based upon the diet program (i.e., a high-fat [F] or normal [N] diet), as follows: F, N, FNF, NNF, FNN, and NNN.

2. Materials and methods

2.1. Reagents

A total of 40 lipid standards were utilized for optimization of nUPLC-ESI-MS/MS run conditions as follows: 16:0-lysophosphatidylcholine (LPC), 17:0-LPC, 12:0/12:0-phosphatidylcholine (PC), 13:0/13:0-PC, 18:1/18:0-PC, 18:0-lysophosphatidylethanolamine (LPE), 17:1-LPE, 12:0/12:0-phosphatidylethanolamine (PE), 14:0/14:0-PE, 17:0/17:0-PE, 18:0/22:6-PE, 18:0p/22:6-PE plasmalogen (PEp), 14:0-lysophosphatidylglycerol (LPG), 17:1-LPG, 18:0-LPG, 12:0/12:0-phosphatidylglycerol (PG), 15:0/15:0-PG, 16:0/16:0-PG, 16:0/18:2-phosphatidylinositol (PI), 17:0/20:4-PI, 17:1-lysophosphatidylserine (LPS), 18:1-LPS, 14:0/14:0-phosphatidylserine (PS), 17:0/20:4-PS, 17:0-lysophosphatidic acid (LPA), 18:0-LPA, 14:0/14:0-phosphatidic acid (PA), 17:0/17:0-PA, 17:0/17:0 D5-diacylglycerol (DAG), 18:1/18:1-DAG, 17:0/17:1/17:0 D5-triacylglycerol (TAG), 54:1(18:0/18:1/18:0)-TAG, d18:1/17:0-Ceramide (Cer), d18:1/22:0-Cer, d18:1/12:0-monohexosylceramide (MHC), d18:1/17:0-MHC, d18:1/16:0-sphingomyelin (SM), d18:1/17:0-SM, d18:1/17:0-sulfatide (ST), and d18:1/24:0-ST. Lipids with odd numbered fatty acyl chains were used as internal standards (ISs) added to brain tissue lipid extracts for targeted quantification. Lipids were purchased from Avanti Polar Lipids Inc. (Alabaster, AL, USA) and Matreya, LLC (Pleasant Gap, PA, USA). HPLC grade solvents (i.e., CH_3OH, H_2O, CH_3CN, isopropanol (IPA), and methyl-*tert*-butyl ether (MTBE)) were purchased from AvantorTM Performance Materials (Center Valley, PA, USA). NH_4HCO_2, NH_4OH, and $CHCl_3$ were purchased from Sigma-Aldrich (St. Louis, MO, USA). Fused silica capillary tubes with inner diameters of 20, 50, and 100 μm (360 μm outer diameter for all) were purchased from Polymicro Technology, LLC (Phoenix, AZ, USA). Packing materials used for LC columns, i.e., Watchers® ODS-P C-18 particles (3 μm and 100 Å), were purchased from Isu Industry Corp. (Seoul, Korea), while 1.7 μm ethylene bridged hybrid (BEH) particles unpacked from ACQUITY UPLC® BEH C18 column (2.1 mm × 100 mm) were purchased from Waters™ (Milford, MA, USA).

2.2. Animals

Four-week-old male C57BL6/N mice were purchased from Central Lab. Animal Inc. (Seoul, Republic of Korea) and maintained in the animal facility at Korea Mouse Phenotyping Center (KMPC), Seoul National University. The animals were housed at 24 ± 2 °C with a 12-h light/dark cycle and fed with a normal diet (NIH-31 chow diet from Zeigler Bros, Inc. (Gardners, PA, USA)) ad libitum, along with tap water, before beginning the dietary experiments. Mice were fed with the dietary programs outlined shown in Fig. 1. For the first 8 weeks, the mice were fed either a normal diet (N group or control-8) or HF diet (F or weight gain-8). For the HF diet, 60% kcal% fat, #D12492 Research Diets (NJ, USA) were used. Details of dietary nutrient composition are in Table S1. For the next 4 weeks, both groups were fed a normal diet. Then, each group was further divided into two sub-groups and fed either a normal or HF diet for 4 weeks. Thus, the 6 groups analyzed in the current study were as follows: N, F, NNN (control-16), NNF (weight gain-16), FNN (weight maintenance), and FNF (weight cycling). Tissue samples from four different brain regions (i.e., the cortex (Co), hippocampus (Hip), hypothalamus (Hyp), and olfactory bulb (OB)) were obtained from the mice (n = 6) at each dietary stage. The animals were sacrificed using CO_2 exposure. All animal experiments in the current study were conducted according to the 'Guide for Animal Experiments,' edited by Korean Academy of Medical Sciences, and were approved by the Institutional Animal Care and Use Committee of Seoul National University (Permit Number: SNU-140205-2-1). Details of extracting mice organs were as follows. Mice were perfused after anesthesia for sample quality control. After removing the blood from the body through perfusion, brain samples were taken immediately. The brain was classified according to the anatomical shape. First, the olfactory bulb was sampled from whole brain followed by the cortex. Hippocampus attached to the cortex was separated and hypothalamus was finally isolated. All the sampling procedures were performed in the same order, and the time difference between each sample was not large because we processed the brain as quickly as possible at the moment of extraction. All samples were placed in liquid nitrogen immediately after removal in order to minimize sample damage. The blood plasma, adipose tissue, and liver were sampled from the same mice. Glucose and cholesterol levels in the blood were measured according to the literature [45].

The weights, blood glucose level, and total cholesterol level of the mice were measured and plotted in Fig. S1 (see Supplementary material). For histopathological examination, each organ was weighed and fixed with 4% paraformaldehyde overnight at room temperature, processed for paraffin sectioning at 4-μm thickness, and stained with hematoxylin and eosin, according to standard procedures. For lipid detection in liver tissue, the sections were washed once with 50% isopropyl alcohol and stained with Oil Red O. Tissue sections were analyzed using an optical microscope equipped with a DP71 digital camera from Olympus (Tokyo, Japan).

2.3. Extraction of lipids from brain tissues

A total of 144 tissue samples (i.e., four different brain regions and six different mice groups, with n = 6 per group) were examined in the current study. Lyophilized brain tissue samples were pulverized into powder to make homogenized mixtures. For non-targeted lipid identification, 0.5 mg of the individual powder tissue sample (n = 6) from each NNN and FNF group were pooled together to make 3 mg of pooled sample for each tissue type. For targeted lipid quantification, 3 mg of a pooled sample for each brain region was used for lipid extraction. Lipid extraction of the tissue samples were conducted by the two stage extraction method with MTBE/CH_3OH [46]. The reason of pooling brain tissues was due to the limited amounts of hypothalamus and olfactory bulb from each animal which were less than minimum weight (3 mg) required for lipid extraction and lipidomic analysis in our lab. The pooled tissue sample (3 mg) was dissolved in 300 μL of CH_3OH and placed in an ice bath for 10 min. MTBE (1 mL) was added to the mixture and vortexed for 1 h. Then, 250 μL of MS-grade H_2O was added and the mixture was vortexed again for 10 min at room temperature. The final mixture was centrifuged at 1000 × *g* for 10 min and the upper organic layer was transferred to a new tube. A total of 300 μL of CH_3OH was added to the remaining lower layer, followed by a tip-sonication for 2 min and centrifugation at 1000 × *g* for 10 min. The resulting organic layer was mixed with the previously collected organic extract. The organic solvent in the mixture was evaporated by vacuum overnight. During evaporation, the tube was wrapped with 0.45 μm MillWrap PTFE membrane from Millipore (Bedford, MA, USA) to minimize the loss of lipids by ejection from the tube. Dried lipids were weighed and dissolved in $CHCl_3$:CH_3OH (2:8, v/v) for storage at −80 °C. For nLC-ESI-MS/MS analysis, each lipid sample was diluted to a lipid concentration of 5 μg/μL in CH_3OH:H_2O (9:1, v/v).

2.4. Nanoflow LC-ESI-MS/MS of lipids

The analytical columns were prepared using a fused capillary tube (100 μm I.D.) by pulling one end of a silica tube with flame to make a sharp needle for a direct ESI emitter. The column was packed with Watchers® ODS-P C18 particles (3 μm), for the first 0.5 cm from the pulled tip to make self-assembled frit, and with BEH particles (1.7 μm), for the remaining 7 cm, under nitrogen gas at 1000 psi. The same column was utilized throughout the experiment for both qualitative and quantitative analyses. The column was connected between the UPLC pump and MS system via PEEK micro-cross from IDEX Health & Science (Oak Harbor, WA, USA), of which three remaining ports were linked to a Pt wire for ESI voltage, a capillary tubing (50 μm I.D.) from UPLC pump, and a pressure capillary (20 μm I.D.), which was connected to an on/off switching valve to split pump flow. The mobile phase solutions for A and B were (9:1, v/v) H_2O:CH_3CN and (2:2:6, v/v/v) CH_3OH:CH_3CN:IPA, respectively, which were added with 0.05% NH_4OH and 5 mM NH_4HCO_2 as the mixed ionization modifier.

We employed two nanoflow LC-ESI-MS/MS systems: one for non-targeted lipid identification and the other for targeted quantitative lipid analysis. In non-targeted analysis, molecular structure of lipid species was identified by collision induced dissociation (CID) experiment. For targeted quantitation, selected reaction monitoring (SRM) method based on triple quadrupole MS system was employed to quantify the selected lipid species based on non-targeted analysis results. A Dionex Ultimate 3000 RSLCnano System with an autosampler coupled with LTQ Velos ion trap mass spectrometer from Thermo Scientific™ (San Jose, CA, USA) was used for non-targeted qualitative lipid analysis. A total of 10 μg of lipid extract sample was loaded to the analytical column with mobile phase A, at 650 nL/min for 10 min, with the switching valve off. Then, the UPLC pump flow rate was increased to 8.5 μL/min, with the switching valve on, so that only 300 nL/min of flow entered the column. A high speed pump flow up to the micro-cross was used to reduce dwell time. Gradient elution-I was initiated by ramping mobile phase B to 55% for 1 min, increasing it to 75% for 10 min, then 85% for 10 min and 99% for 15 min, before being maintained at 99% for 10 min. It was then decreased to 1% B and re-equilibrated for 10 min before the next run. The ESI voltage was set to 3.0 kV and 40% normalized collision energy was used for data dependent CID analysis. The *m/z* range of a precursor MS scan was 300–1200 amu. The lipids were identified by LiPilot, a computer software program that determines lipid molecular structures from CID spectra, which was developed in our laboratory [47].

A nanoACQUITY UPLC system with an autosampler from Waters™ (Milford, MA, USA), equipped with a TSQ Vantage triple-stage quadrupole MS system from Thermo Scientific™, was used with the SRM method for targeted quantification of lipids. The lipid extract sample for quantification was added with a mixture of 18 ISs (1 pmol each per 10 μg of each lipid extract sample) and the mixture was loaded to the

analytical column (same as the above) at 1 μL/min using mobile phase A for 10 min. During lipid quantification, the pump flow rate was set to 15 μL/min with the split valve on and the column flow rate was adjusted to 300 nL/min by controlling the length of pressure capillary tube. Gradient elution-II was initiated with the mobile phase B to 60% for 1 min, ramped to 75% for 2 min, 80% for 3 min, 90% for 5 min, and then to 100% for 5 min. It was maintained at 100% B for 10 min and resumed to 100% A for 5 min of column re-conditioning. SRM-based quantification was performed by analyzing precursor and product ions in data-dependent CID experiments. The SRM analysis was accomplished in positive and negative ion modes alternatively, using a scan width at m/z 1.5, scan time at 0.001 s, and ESI voltage of 3 kV. The LPC, PC, LPE, PE, PEp, DAG, TAG, Cer, SM, MHC, and ST lipid classes were analyzed in the positive ion mode, while the LPG, PG, LPI, PI, LPS, PS, LPA, and PA were analyzed in the negative ion mode. The CID energy specific to lipid class was as follows: 20 V for LPE, PE, and Pep; 25 V for DAG and TAG; 30 V for Cer and MHC; 35 V for LPG, PG, LPI, PI, LPS, PS, LPA, and PA; 40 V for LPC, PC, and SM; and 50 V for ST. Lipids were quantified by calculating the corrected peak area, i.e., the ratio of peak area of a species to that of the IS specific to each lipid class. Since the concentration of each IS was adjusted to 1 pmol per injection, the corrected peak area value of each lipid molecule was considered as close to the pmol amount under the assumptions that MS intensity of lipids in this study was not significantly affected by the length of acyl chain and degree of unsaturation. The statistical analyses of the data were performed with Student's *t*-test using SPSS software (version 20.0, IBM Corp., Armonk, NY, USA), and principal component analysis (PCA) using Minitab 17 statistical software (http://www.minitab.com).

3. Results

3.1. Weight change and histology

The change in body weight plotted in Fig. S1a, demonstrated weight gain in mice fed with a HF diet (i.e., in the F, NNF, and FNF, groups). The FNN group gained weight from 20.8 g to 43.6 g during the first 8 weeks of HF diet, and then reduced to 34.0 g during the normal diet for 8 weeks, eventually recovering to a weight similar to that of NNN. A characteristic result was that mice in the FNF, in particular, gained more weight than those in the NNF group that did not undergo weight loss before the HF diet. When the FNF group undergoing HF diet for the first 8 weeks were compared with the NNFs that had a normal diet, the final weight of the FNF was 46.3 g and the NNF was 42.2 g, which showed a large difference ($p < 0.05$). Therefore, it can be thought that the influence of yo-yo phenomenon was critical. The levels of fasting blood glucose and total cholesterols were significantly increased in the FNF group more than in the NNF group, as shown in Fig. S1b and S1c. Moreover, histopathological examination of liver sections revealed that FNF mice accumulated lipid droplets, resembling macro- and microvesicular steatosis, in their livers (Fig. S1d and S1e). In addition, the size of the adipocytes was significantly increased in the FNF group compared to the NNF group (Fig. S1f). Taken together, these findings demonstrated that weight regain after weight loss negatively affected metabolic health, in comparison to simple weight gain.

3.2. Lipid profiling in brain tissue

From non-targeted lipid analysis of the four brain regions, a total of 359 lipids from 19 lipid classes, including PLs, LPLs, PEp, DAG, TAG, ST, SM, and Cer were identified with individual molecular structures using nUPLC-ESI-MS/MS. Representative base peak chromatograms of the tissue samples from the NNN (control) and FNF (weight cycling) groups, shown in Supplementary Fig. S2, demonstrate significant differences in peak profiles between the two extreme diet groups. The performance of lipid separation employed in this nUPLC experiment was demonstrated by the separation of lipid standards in both positive and negatives ion mode during MS detection (Fig. S3). The run conditions that were employed offered high-resolution separation, which enabled regioisomers of each lysophospholipid (peaks 1–2 in positive and peaks 1–4 in negative ion runs) to be distinguished (Fig. S3). The measured peak widths of entire lipid standards were 0.4–0.8 min. Molecular structures of identified lipids from brain tissues are listed in Table S2. Among the 359 lipids, SRM quantitation was only conducted for 270 lipids, since the PC, PE, and TAG lipid classes were quantified without differentiating the isomeric combinations of acyl chains. Therefore, chain structures of these three classes are represented as the total number of carbons and double bonds in acyl chain, as listed in Table S2. The detailed chain structures of the geometric isomers, based on CID experiments, are listed in Table S3. High-speed targeted quantitation of lipids was conducted by monitoring a precursor ion of each lipid class and its corresponding product ion as a quantifier ion, utilizing an SRM time-table in which a detailed inclusion list was made to scan every lipid molecule within a 2-min interval during the gradient nUPLC separation. The types of precursor and quantifier ion for each lipid class are listed in Table S4. The number of identified and quantified lipids as well as the molecular structures of 19 internal standards, which were specific to each class and used to calculate the corrected peak area of each lipid species, are also listed. Since the amount of each IS added to each injection was 1 pmol, the corrected peak area of each lipid species listed in Table S2 represent the approximate value at pmol level, with an assumption that the effects of the length and degree of unsaturation of acyl chains on MS intensity of lipids were minimized at such low concentration levels [48]. The relative abundance of lipid species were provided for N and NNN groups alone and calculated within each lipid class. Lipid species with a bold number of relative abundance represents high-abundance species in each class, which were defined as having a percentage value larger than 100/number of lipids in each class.

Lipidomic differences in the mouse brain tissue were examined by comparing the overall levels of each lipid class as listed in Table S5. The level of each lipid class is the summed value of corrected peak areas of individual lipids (relative to 1 pmol of each IS) per each injection (10 μg injection equal to 40 μg of tissue). As seen in Table S5. PI and PC were highly abundant in the four brain regions examined in the current study, followed by MHC and PE. This is clearly noted in the number scales of corrected peak area plot (y-axis) of each lipid class shown in Fig. 2 which shows the differences in the overall levels of these lipid classes along with the compositional variations among tissues of which the numbered individual lipids are relatively abundant in each class and their molecular structures are listed in Table S6. The levels of ST, SM, and PG appeared to be approximately 10–15-fold less abundant than those of PC and PI. It is unique that the PI species were highly abundant in brain tissue, compared to previously reported PI levels in the lung or muscle tissue [43,49]. Significant differences (> 2-fold) in the composition of lipid classes were found between the four regions, in control mice (N), as marked in bold for the seven lipid classes (i.e., MHC, PEp, PA, TAG, ST, DAG, and SM) in Table S5 and in Fig. 2. In Fig. 2, the levels of MHC, PEp, TAG, ST, and DAG are exclusively higher in the hypothalamus than in other tissues and the level of PA in hippocampus appear to be 2–3 times less abundant than in the others. However, other highly abundant lipid classes such as PC and PE show similar lipid levels among tissues except PI (1.5–2 times larger in hypothalamus and olfactory bulb) in Fig. S4.

3.3. Effect of HF diet on brain lipids

Alterations in lipid profiles during the different diet programs were analyzed using the PCA for the quantified results of 270 lipids from the six mouse groups. Fig. 3 shows the PCA plots representing the differences in lipid profiles in the four brain regions among the mice from the six different diet programs. Data points from mice with normal diet (i.e., the N, FNN, and NNN groups) were clustered and clearly apart

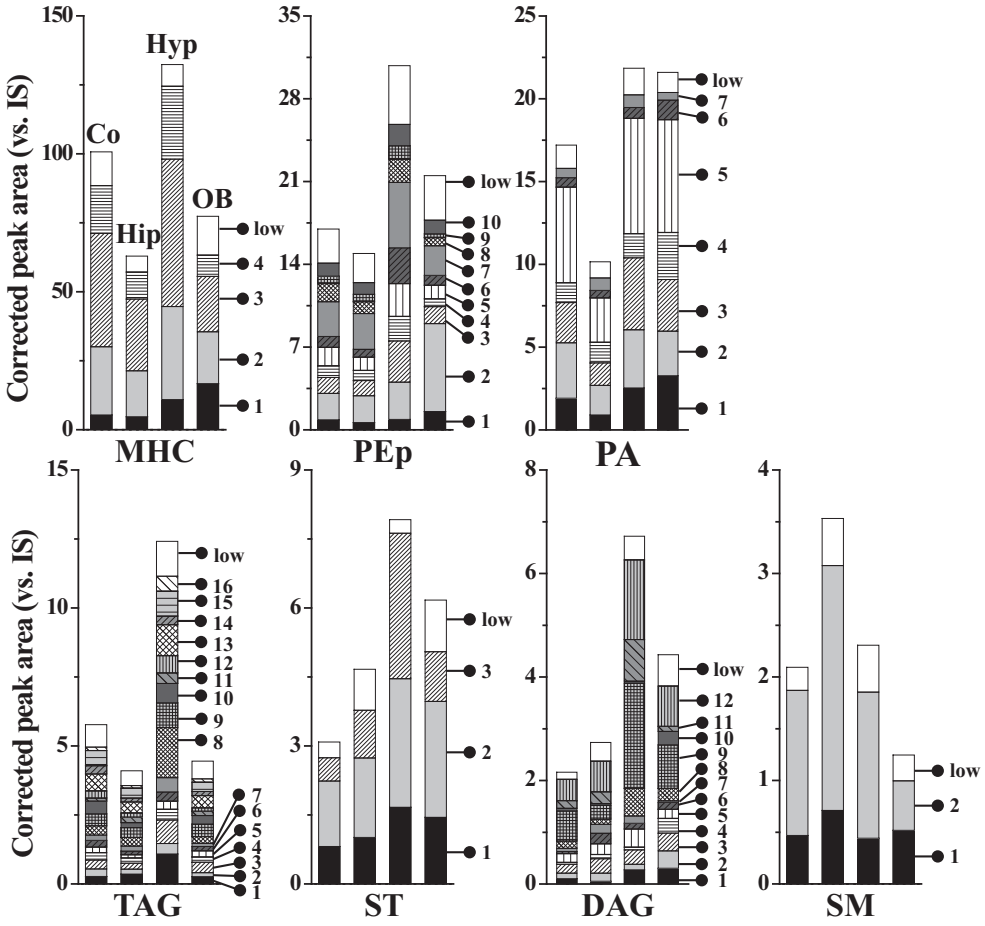

Fig. 2. Compositional differences in lipids among the four brain regions (i.e., Co, Hip, Hyp, and OB) of 8 weeks control (N) mice for the seven lipid classes (MHC, PEp, PA, TAG, ST, DAG, and SM), which showed more than a 2-fold change among the four tissue types obtained by nUPLC-ESI-MS/MS. The number marked for each bar represents an individual lipid molecule, species with relatively high abundance are listed in Table S6. The "low" represents the summed amount of the low abundance species.

from those with an HF diet (i.e., the F, NNF, and FNF groups) for analyzed brain regions. Data points from the cortex and hippocampus were clustered very closely, implying that lipid patterns in these two regions were similar to each other. Although differences between the cortex and hippocampus were not obvious, these patterns were clearly clustered apart from those of the olfactory bulb and hypothalamus. Fig. 3 supports that the lipid profiles with a normal diet were clearly different from those associated with an HF diet in every brain region that was analyzed.

To clearly elucidate the difference between the HF diet groups and normal diet groups, the volcano plots ($\log_{10}$ (p value) vs. $\log_2$ (fold change)) of 270 quantified lipid species are shown in Fig. 4 for cortex and hippocampus, and in Fig. S5 for hypocampus and olfactory bulb. The two vertical lines in each plot represent 3-fold changes between HF diet groups and normal diet groups (F vs. N, NNF vs. NNN, and FNF vs. NNN). The volcano plots show that significant number of species were influenced in HF diet > 3 fold increases.

As seen in Fig. 5 significant changes in tissue-specific lipid profiles among different diet programs were observed for several lipid classes (> 3-fold, $p < 0.001$). Fig. 5 shows that the HF diet significantly increased the level of DAG in all analyzed regions, in the F (vs. N) and FNF (vs. both NNN and FNN groups) groups. Further, the Cer level in the olfactory bulb and cortex in the FNF was also elevated. Moreover, the levels of LPC, LPE, LPG, LPS, and LPA in the cortex of mice in the FNF group were significantly (> 3-fold) increased (Fig. 5c), while the levels of PE, PEp, LPC, and LPE in the hippocampus in mice in the F group were increased by > 3-fold (Fig. S6). These results indicated that while the HF diet affected lysophospholipids in both the cortex and hippocampus, it did not have much of an effect on those in the hypothalamus and olfactory bulb.

Fig. 6 outlines the variations at the molecular level, in the four brain regions, using a heat map of the 82 individual lipid molecules that exhibited significant changes (> 3-fold and $p < 0.001$), either in the NNF or FNF group, respectively, in comparison to the NNN group. The heat map shows clear differences between the normal diet groups (i.e., the N, NNN, and FNN groups) and the HF diet groups (i.e., the F, NNF, and FNF groups). The increased patterns appear to be larger in the cortex and hypothalamus, compared to that in the other two regions.

While Fig. 5 shows the significant increase in DAG (> 3-fold, $p < 0.001$) in the four brain regions, Fig. 7 shows changes (FNF/NNN) in the level of high abundant DAG species, along with two Cer species (d18:1/24:0 and d18:1/24:1). These results demonstrated that DAGs were the lipid species that were most influenced by the HF diet, without noticeable differences among individual species.

Although the HF diet seemed to increase most species, two PS species (i.e., 18:0/22:6 and 18:1/22:6) in the heat map of Fig. 6 appeared to decrease in the cortex and hippocampus. Further investigations on the variation of PS in relation to LPS, indicated that the decrease of PS molecules resulted in the increase of LPS in the cortex and hippocampus. Fig. 8a plots the overall and individual levels of highly abundant PS and LPS species in the cortex of mice in the FNN, NNF, and FNF groups in comparison to the NNN group. Overall, there was no change in the PS and LPS levels of the FNN group (vs. NNN), supporting that the levels of these lipid in weight loss group (FNN) recovered to the

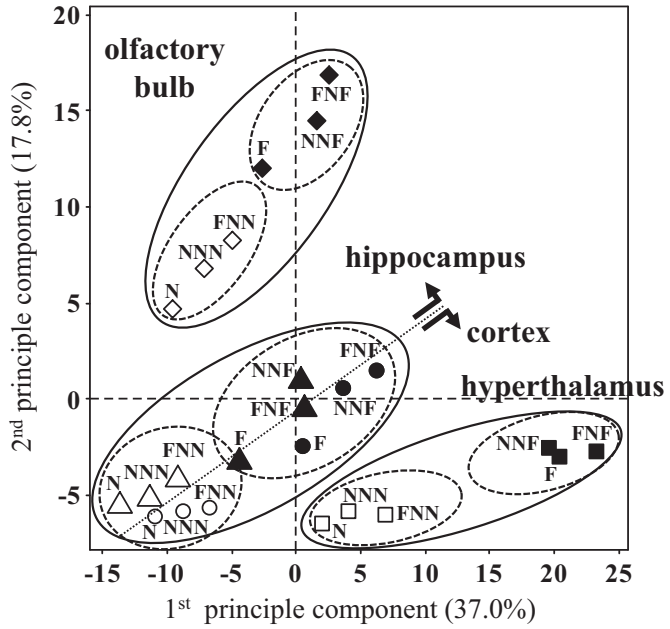

Fig. 3. Principal component analysis (PCA) plots representing the difference among the six mice groups (i.e., N, F, NNN, FNN, NNF and FNF), for each brain region, based on quantified results of 270 lipids. Data for the normal (N) and HF diet are shown by open and filled shapes, respectively. Data from the cortex, hippocampus, hypothalamus, and olfactory bulb are shown indicated circles, triangles, rectangles, and diamonds, respectively.

NNN level after switching to a normal diet. The levels of PS lipids in the NNF and FNF groups, however, were decreased by approximately 2-fold in the cortex, while LPS levels were increased by 2–3-folds. These changes could be primarily attributed to the decrease in highly abundant PS molecules with acyl chains of 16:0, 18:0, 18:1, and 22:6. A detailed plot for the cortex is shown in Fig. S7a, showing significant decreases (of > 2-fold; represented by an asterisk) of highly-abundant PS lipid species marked with * (i.e., 16:0/22:6, 18:0/22:6, and 18:1/22:6). These decreases appeared to increase of LPS species containing the same common chains (i.e., 16:0, 18:0, and 22:6), supporting that highly abundant PS lipids were converted to LPS either by oxidative or enzymatic dissociation. This is related to the oxidative cleavage of an acyl chain of PLs, which primarily occurs with unsaturated acyl chains.

The degree of LPS increase in the cortex was larger in the FNF group than in the NNF group. Similar results are demonstrated in the hippocampus (Fig. S7b) and hypothalamus (Fig. S7c). However, no noticeable change in the PS and LPS levels (both overall and in highly abundant species) in the olfactory bulb (Fig. 8b; also see detailed plots in Fig. S7d).

3.4. Effect of weight cycling on brain lipids

Although the differences between the two mouse groups that terminated with the HF diet (FNF and NNF) were not apparently large in the heat map, the differences in the lipid profiles between the two groups were interesting to trace the weight cycling effect, which is known as the yo-yo effect. Fig. 9 shows the ratio (FNF/NNF) of 14 lipid species that showed a significant change of > 1.5-fold ($p < 0.01$) in the cortex, hippocampus, and olfactory bulb. Even with this mild screening, none of lipid species in the hypothalamus showed a meaningful difference upon weight cycling. Although the levels of two TAGs

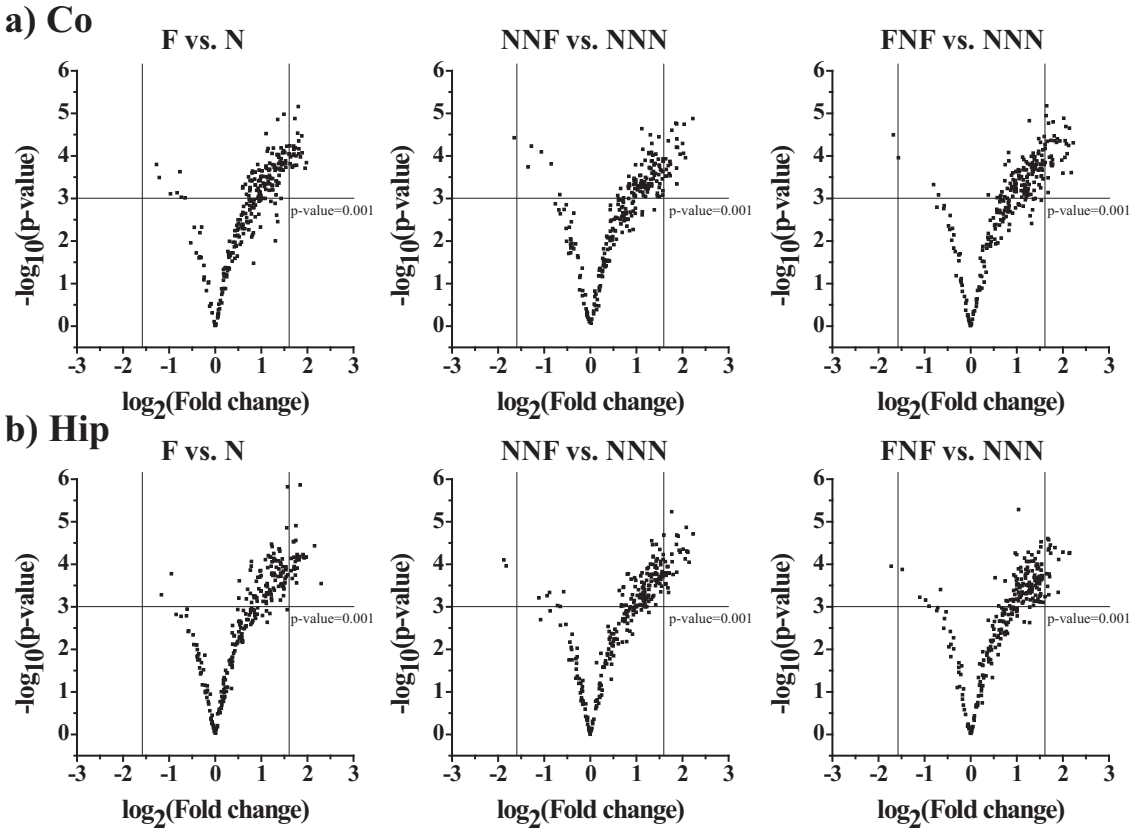

Fig. 4. Volcano plots of 270 lipids species showing the difference between the HF diet groups and normal diet groups from a) cortex and b) hippocampus. The x-axis was divided into two sections so as to represent the value over than 1.585 or less than −1.585. The y-axis segmented based on the p-value = 0.001 between two groups.

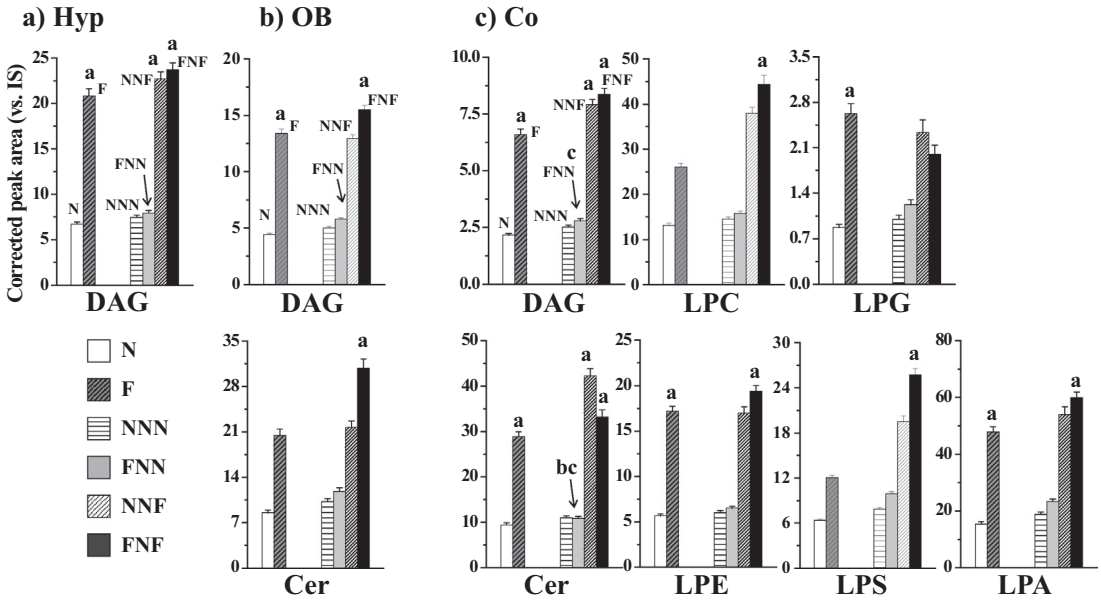

Fig. 5. Overall amount of lipid classes showing a significant change (> 3-fold and $p < 0.001$ marked with a: vs. N or NNN; b: vs. NNF; c: vs. FNF) in the a) hypothalamus (Hyp), b) olfactory bulb (OB), and c) cortex (Co) of mice in the six groups (N, F, NNN, FNN, NNF, and FNF).

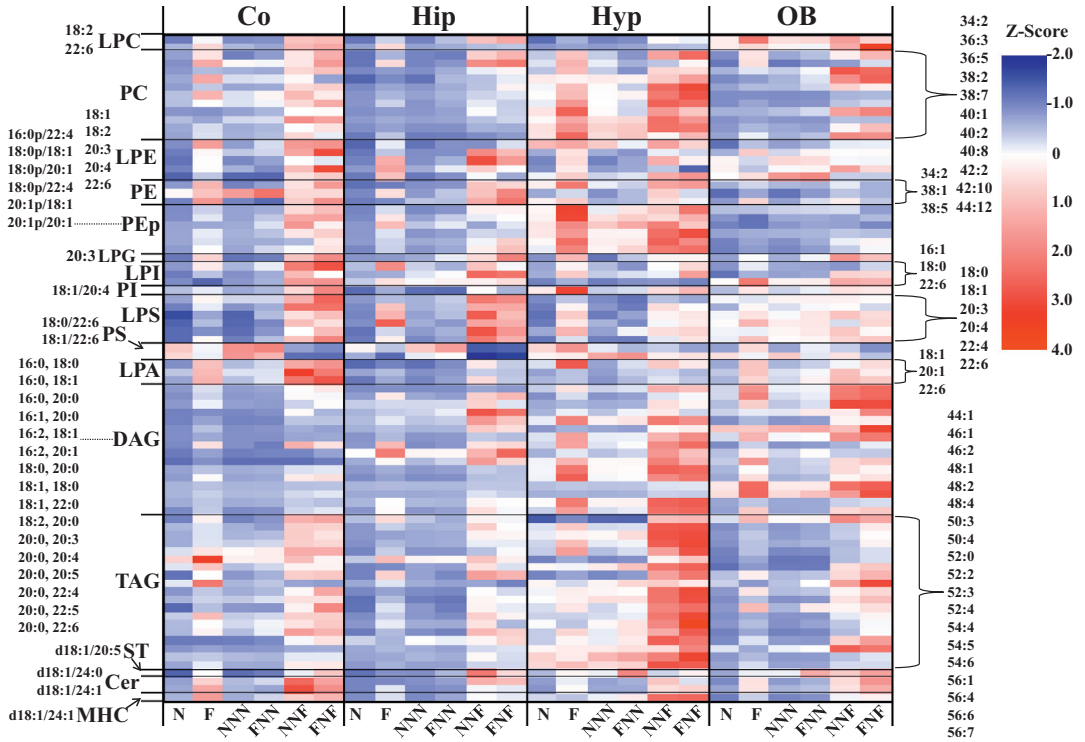

Fig. 6. Heat map of 82 lipid species showing significant changes (> 3-fold, $p < 0.001$), compared to the NNN group, in the four different brain regions (i.e., cortex [Co], hippocampus [Hip], hypothalamus [Hyp], and olfactory bulb [OB]), either in the NNF or FNF groups.

(52:2 and 52:4), 20:4-LPE, and 18:1/20:4-PI were further elevated in the cortex, with weight cycling, it should be noted that 18:0p/20:1-PE and 18:0-LPI were decreased. In the hippocampus, the species that showed a significant change were found to decrease, except 38:7-PC. In the olfactory bulb, however, the weight cycling effect elevated all four species (i.e., 22:6-LPC, 42:10-PC, 46:1-TAG, and d18:0/24:0-Cer). The lipids that showed an overall significant change ($p < 0.01$) are listed in Table 1. A total of 10 (of 16), 2 (of 14), 2 (of 4), and 9 (of 9) lipids were significantly elevated in the cortex, hippocampus, hypothalamus, and olfactory bulb in the FNF group than in the NNF, respectively. Although the ratio of FNF/NNF did not show significant alterations at the molecular level, the change in the levels of each lipid class are readily recognized in the plots of Fig. 5, which demonstrated that the lipid accumulation of some classes, such as DAG and Cer in the olfactory bulb, LPS in the cortex, and PEp in the hippocampus, was accelerated by the yo-yo effect.

4. Discussion

In this study, six different diet groups from four different regions of

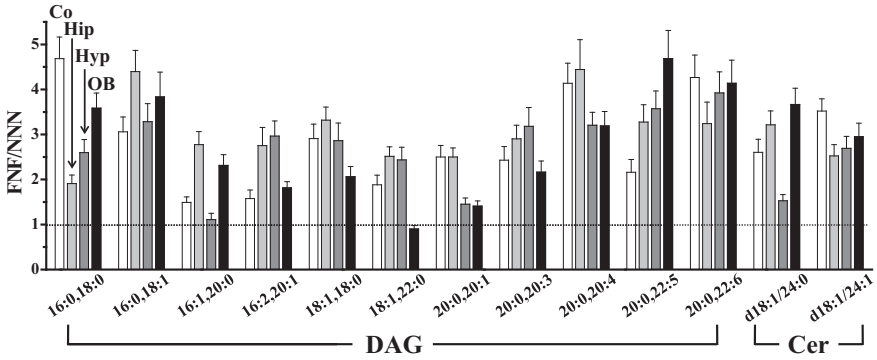

Fig. 7. Change in the amount of highly abundant diacylglycerol (DAG) and ceramide (Cer) species in the FNF group compared to those in the NNN group.

brain were analyzed. In phenotypic outcomes, FNF mice gained more weight than the NNF group that did not undergo weight loss before HF diet. The weight of liver and the size of adipocyte were significantly increased in the FNF group compared to those in the NNF group. Moreover, lipid droplets and triglyceride contents in the liver of FNF were highly accumulated, and the levels of fasting blood glucose and total cholesterol were significantly increased in the FNF group. In summary, these findings indicate that weight regain (FNF) after weight loss affects metabolic dysfunction as compared to weight gain (NNF).

In the lipidomic study, comprehensive profiling of brain lipids (270 quantified out of 359 identified lipids), following various diet programs, was accomplished for four different regions in the mouse brain, using nUPLC-ESI-MS/MS. Examinations on the compositional variations of lipids among the four brain regions of mice with normal diet revealed that the MHC, PEp, TAG, DAG, and ST lipid classes were enriched in the hypothalamus, while the olfactory bulb was rich in PS and PG. The PCA analysis demonstrated that the effect of the HF diet on individual lipid levels depended of the brain region, except in the cortex

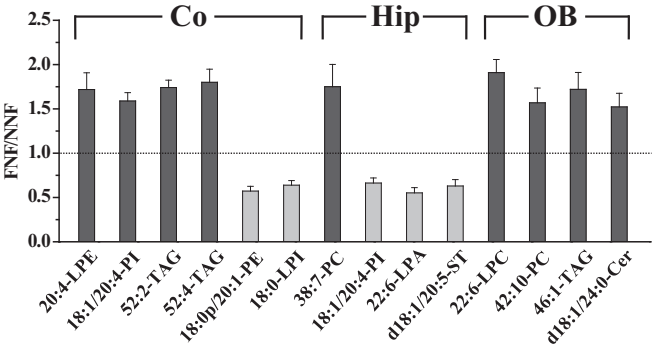

Fig. 9. Ratio (FNF/NNF) of lipid species in the heat map showing significant changes ($p < 0.01$ in FNF vs. NNF) in the a) cortex (Co), b) hippocampus (Hip), c) hypothalamus (Hyp), and d) olfactory bulb (OB).

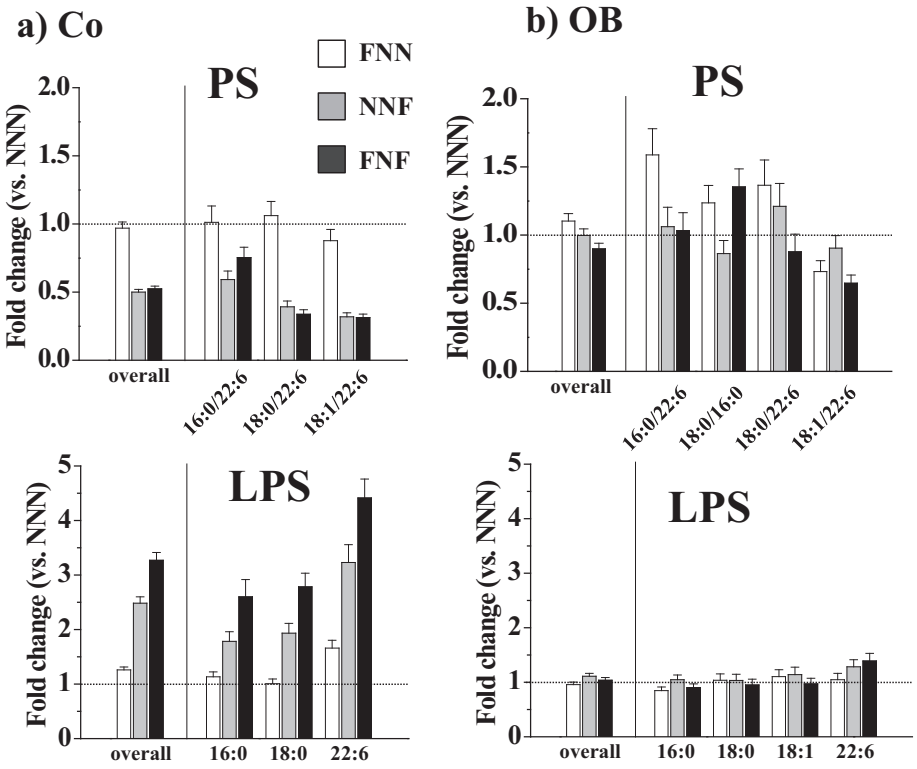

Fig. 8. Changes in the overall phosphatidylserine (PS) and lysophosphatidylserine (LPS) levels and of relatively highly abundant individual PS and LPS molecular species in the a) cortex and b) olfactory bulb. Fold change of the FNN, NNF, and FNF groups are represented vs. NNN group.

Table 1
Ratio (FNF/NNF) of lipid species showing a significant change ($p < 0.01$, FNF vs. NNF; shown in bold) in the a) cortex, b) hippocampus, c) hypothalamus, and d) olfactory bulb. The relative abundance (%) of each lipid class is denoted and highly abundant species has been underlined.
F, high-fat diet; N, normal diet.

Class	Molecular species	*m/z*	FNF/NNF							
			%	Co	%	Hip	%	Hyp	%	OB
LPC	22:6	568.5	23.5	1.12 ± 0.15	17.2	1.13 ± 0.15	6.3	1.07 ± 0.17	23.1	**1.91 ± 0.15**
PC	38:2	814.5	1.3	0.6 ± 0.07	0.6	1.21 ± 0.11	1.4	1.28 ± 0.18	1.2	**1.18 ± 0.05**
	38:7	804.5	0.1	1.08 ± 0.1	0.0	**1.75 ± 0.25**	0.1	1.16 ± 0.1	0.1	0.78 ± 0.13
	40:2	842.5	0.2	1.43 ± 0.13	0.1	**0.79 ± 0.05**	0.2	0.93 ± 0.1	0.1	1.21 ± 0.13
	42:10	854.5	0.1	1.29 ± 0.19	0.1	0.99 ± 0.16	0.2	0.97 ± 0.14	0.1	**1.57 ± 0.17**
LPE	18:2	478.5	0.6	**1.49 ± 0.19**	0.4	**0.77 ± 0.07**	0.3	0.88 ± 0.09	0.3	1.02 ± 0.09
	20:3	504.5	1.0	0.91 ± 0.14	1.1	**0.73 ± 0.07**	0.5	**0.69 ± 0.02**	1.1	0.99 ± 0.1
	20:4	502.5	25.2	**1.72 ± 0.19**	24.6	0.72 ± 0.09	11.6	0.3 ± 0.03	15.7	0.71 ± 0.07
PE	34:2	716.5	0.1	**1.44 ± 0.15**	0.2	0.91 ± 0.11	0.3	1.05 ± 0.13	0.3	0.79 ± 0.08
	38:5	766.5	3.4	**1.36 ± 0.1**	6.8	1.28 ± 0.15	6.1	0.8 ± 0.1	6.6	0.74 ± 0.08
Pep	18:0p/20:1	758.5	4.8	**0.57 ± 0.05**	7.9	1.58 ± 0.18	6.6	0.67 ± 0.08	3.0	0.76 ± 0.09
	20:1p/20:1	784.5	0.1	1.3 ± 0.23	0.2	**1.41 ± 0.15**	0.2	1.05 ± 0.17	0.1	1.31 ± 0.14
LPI	18:0	599.5	16.6	**0.64 ± 0.05**	27.4	0.96 ± 0.08	23.7	1.97 ± 0.19	14.8	0.97 ± 0.08
PI	18:1/20:4	883.5	9.0	**1.59 ± 0.1**	5.7	**0.66 ± 0.06**	7.7	1.24 ± 0.13	7.5	0.96 ± 0.09
LPS	22:4	572.5	3.2	**1.46 ± 0.12**	4.9	**0.77 ± 0.06**	5.9	1.06 ± 0.09	3.4	0.75 ± 0.08
	22:6	568.5	26.3	**1.37 ± 0.14**	28.6	**0.75 ± 0.05**	30.4	1.3 ± 0.15	23.6	1.08 ± 0.1
LPA	18:1	435.5	18.8	1.12 ± 0.13	14.9	**0.68 ± 0.08**	18.9	0.82 ± 0.07	14.5	1.3 ± 0.11
	20:1	463.5	2.5	**0.77 ± 0.06**	1.7	0.92 ± 0.1	1.4	0.74 ± 0.07	2.0	0.7 ± 0.06
	22:6	481.5	40.4	1.14 ± 0.12	34.6	**0.55 ± 0.06**	30.4	0.83 ± 0.07	38.7	0.89 ± 0.07
DAG	16:2,18:1	608.5	0.4	0.99 ± 0.11	1.3	**0.72 ± 0.08**	0.9	0.88 ± 0.11	0.3	1.08 ± 0.12
	18:1,18:0	640.5	7.4	**0.73 ± 0.08**	5.9	1.06 ± 0.12	5.1	1.15 ± 0.15	3.9	1.47 ± 0.16
	18:1,22:0	696.5	2.0	1.61 ± 0.16	7.4	1.52 ± 0.11	1.8	**0.76 ± 0.07**	3.2	0.97 ± 0.09
	18:2,20:0	666.5	0.3	1.74 ± 0.21	0.9	**0.67 ± 0.08**	0.6	0.74 ± 0.09	0.6	1.15 ± 0.12
	20:0,20:4	690.5	29.5	1.12 ± 0.1	9.7	1.04 ± 0.1	28.5	1.14 ± 0.12	19.0	**1.23 ± 0.1**
	20:0,22:6	714.5	17.3	1.15 ± 0.12	21.8	**0.69 ± 0.09**	23.1	1.04 ± 0.11	17.5	1.15 ± 0.12
TAG	46:1	794.5	3.7	0.97 ± 0.12	4.7	0.68 ± 0.08	2.7	1.01 ± 0.13	3.5	**1.72 ± 0.19**
	48:4	816.5	0.2	0.69 ± 0.08	0.3	0.74 ± 0.08	0.0	**1.36 ± 0.15**	0.1	1.23 ± 0.13
	52:0	880.5	1.3	0.94 ± 0.12	1.5	0.64 ± 0.07	1.0	0.84 ± 0.08	1.9	**1.47 ± 0.13**
	52:2	876.5	8.3	**1.74 ± 0.08**	7.4	0.82 ± 0.08	7.5	1.17 ± 0.14	13.0	1.22 ± 0.14
	52:4	872.5	0.8	**1.8 ± 0.15**	1.1	0.85 ± 0.1	0.6	1.11 ± 0.12	1.4	1.16 ± 0.16
	54:5	898.5	10.9	1.22 ± 0.14	9.4	0.47 ± 0.06	7.2	**1.5 ± 0.16**	6.5	1.4 ± 0.21
	56:1	934.5	0.0	1.31 ± 0.14	0.2	1.29 ± 0.13	0.1	0.9 ± 0.11	0.1	**1.38 ± 0.11**
	56:6	924.5	0.4	1 ± 0.12	0.5	0.7 ± 0.09	0.8	1.32 ± 0.16	0.2	**1.44 ± 0.15**
ST	d18:1/20:5	824.5	39.0	**1.42 ± 0.16**	38.5	**0.63 ± 0.07**	33.8	1.25 ± 0.15	35.7	1.23 ± 0.16
Cer	d18:1/24:0	650.5	26.5	**0.76 ± 0.06**	29.7	0.93 ± 0.1	20.5	0.59 ± 0.06	21.8	**1.52 ± 0.15**
	d18:1/24:1	648.5	56.6	**0.75 ± 0.06**	52.5	0.93 ± 0.09	46.3	1.1 ± 0.11	60.1	1.43 ± 0.13

and hippocampus, which showed overall similarity. It was evident that the first 8-weeks of an HF diet increased most classes of lipids by 2–3-fold (F vs. N), with greater changes in the cortex and hippocampus, than in the olfactory bulb and hypothalamus. However, the total amounts of each lipid class reverted to the levels seen in the N group, after a return to two consecutive 4-week normal diet periods (i.e., the FNN group). This suggested that the lipid profiles recovered well, regardless of a previous HF diet experience. When 4 weeks of normal diet were followed by 4 weeks of an HF diet, to both the initial N and F groups, it was surprising that the levels of the same lipid classes (i.e., in the NNF and FNF groups) were ramped to similar levels or even higher of the F group. Among the lipid classes, DAG showed a trend of increasing in all four analyzed regions, while Cer was significantly increased in the cortex and olfactory bulb. A recent study demonstrated that the HF diet increased the levels of DAG and Cer in the mouse brain, as well as in the pancreas, liver, and muscle [33]. Since an HF diet or overnutrition causes an increase of intracellular DAG and Cer levels, which are known to block insulin signaling in skeletal muscle and liver [50], it can be expected that an HF diet would also lead to a substantial increase in the level of DAG in the brain tissue, like in our study. This was closely related to the DAG-induced insulin resistance in the muscle [51] and brain [52]. In our studies, the PC levels in the hippocampus and olfactory bulb were increased by weight cycling. (Fig. 9). It was reported that PC levels were significantly increased in the cerebrospinal fluid of patients with amyotrophic lateral sclerosis (ALS) and the brain of mouse groups with ALS, the commonest adult-onset motor neuron disorder characterized by the degeneration of motor neurons in the brain and spinal cord [53].

On the other hand, it is interesting that the various brain regions have different lipid composition. The brain is particularly enriched in lipids with a more diverse lipid composition than other tissues [54]. Lipids play critical roles in various biological processes and functions in brain, including membrane formation and trafficking, signal transmission, and synaptogenesis [55]. Brain contains three major classes of lipids: phospholipid, sphingolipid, and cholesterol. While phospholipids form the backbone of neural membranes [56], sphingolipids that are enriched in neuronal membranes participate in the development and differentiation of neurons [57]. The altered lipid profiles from different areas of the brain can offer clues to metabolic controls related with cell signaling. Brain cholesterol is an essential component not only in structuring cellular membrane and myelin, but also in synapse formation, dendrite differentiation, axonal elongation, and long-term potentiation [58]. Taken together, the changes in lipid compositions in various regions of the brain appear to be due to the differences in distribution, development and differentiation of neurons including myelin sheaths, synapse, dendrite, and axon.

It is noteworthy that although the HF diet increased most lipids, it decreased most PS species. The alterations in highly abundant PS species are likely to be correlated with LPS. Although the HF diet decreased the levels of highly abundant PS species, containing an acyl chain of 16:0, 18:0, and 22:6, by approximately 2-fold, in the cortex, hippocampus, and hypothalamus, in the NNF and FNF (vs. NNN) groups, the LPS species with these acyl chains were significantly elevated. However, this correlation was not observed in the olfactory bulb, as LPS

levels remained unchanged in the olfactory bulb. LPS is produced by the oxidation of PS molecules by an enzyme or oxidant. The emerging roles for LPS include the resolution of inflammation as well as the promotion of phagocytosis of apoptotic cells [59]. Thus, the decrease in PS levels with the substantial increase in LPS (with the same acyl chains) can be expected due to the increase in oxidative stress and inflammation caused by the HF diet.

Overall, the final 4 weeks of the HF diet had a critical impact on the perturbation of brain lipid profiles in the mouse group that experienced an 8-week HF diet first (i.e., the FNF group). In contrast to those in the NNF group, the 14 individual lipids of the FNF group that were significantly increased (> 1.5-fold, $p < 0.01$), demonstrated the accelerated accumulation of certain lipids due to the yo-yo effect. These results implied that mice preceded with HF diet would be affected by the HF diet more than those without it. This might be attributed to adipose cellularity because adipocyte hypertrophy and the number of adipocytes increased by obesity, however hyperplasia was maintained even after weight loss. Furthermore, the obesity might cause permanent changes in brain reward circuitry [60]. The HF diet can naturally cause obesity and affect not only adipocytes but also non-adipocytes including brain tissue, therefore, FNF was more affected than NNF. HF diet and obesity are well known risk factors for the development of neurodegenerative disease such as dementia [61,62]. HF diet-induced damages to the brain are oxidative stress, insulin resistance, inflammation, and changes in blood-brain barrier (BBB) integrity [63]. HF diet was reported to result in obesity-induced hypothalamic neuroinflammation and increased BBB permeability in cortex and hippocampus, and BBB leakage was found as a contributing factor to obesity-induced neuroinflammation and cognitive deficits [64,65]. Administration of HF diet to rats was reported to induce a decrease of haptoglobin (Hpt) level which acts as an antioxidant by binding with free haemoglobin (Hb) in hippocampus, resulting in the increase of protein oxidative modification and neuroinflammation [66]. The latter strongly suggested that Hpt secretion can be interrupted by the alteration in brain lipid compositions.

Although the current study was confined to analyze lipids from a pooled tissue sample of each group due to the limitations in the amount (< 3 mg) of hypothalamus and olfactory bulb of mouse, an insight on biological replicates was not included. However, the present experiments revealed not only the compositional differences of lipid molecular distributions among four different brain regions, but also the fact that the HF diet induced significant increases in the brain lipid levels. Moreover, these results demonstrated that weight cycling may induce the accelerated accumulation of a few lipids in the brain tissue.

Author contributions

J. C. Lee and S. M. Park carried out the lipidomic analysis. I. Y. Kim, and H. Sung performed animal experiments. J.K. Seong designed the animal experiments. M.H. Moon supervised lipidomic analysis and wrote the manuscript. All the authors discussed and approved the final manuscript.

Conflict of interest

The authors have no conflicts of interest to declare.

Transparency document

The Transparency document associated with this article can be found, in online version.

Acknowledgements

We would like to thank the Korean Mouse Phenotyping Center for providing the mouse samples.

Funding

This work was supported by a grant (NRF-2015R1A2A1A01004677) and by the Bio & Medical Technology Development Program (NRF-2013M3A9B6046413) through the National Research Foundation (NRF) of Korea, funded by the Ministry of Science, ICT & Future Planning.

Appendix A. Supplementary data

Supplementary data to this article can be found online at https://doi.org/10.1016/j.bbalip.2018.05.007.

References

[1] M.R. Wenk, The emerging field of lipidomics, Nat. Rev. Drug Discov. 4 (2005) 594–610.
[2] A. Bosio, E. Binczek, W. Stoffel, Functional breakdown of the lipid bilayer of the myelin membrane in central and peripheral nervous system by disrupted galactocerebroside synthesis, Proc. Natl. Acad. Sci. U. S. A. 93 (1996) 13280–13285.
[3] K. Eisinger, G. Liebisch, G. Schmitz, C. Aslanidis, S. Krautbauer, C. Buechler, Lipidomic analysis of serum from high-fat diet induced obese mice, Int. J. Mol. Sci. 15 (2014) 2991–3002.
[4] C.L. Kien, J.Y. Bunn, M.E. Poynter, R. Stevens, J. Bain, O. Ikayeva, et al., A lipidomics analysis of the relationship between dietary fatty acid composition and insulin sensitivity in young adults, Diabetes 62 (2013) 1054–1063.
[5] P.G. Meikle, G. Wong, C.K. Barlow, B.A. Kingwell, Lipidomics: potential role in risk prediction and therapeutic monitoring for diabetes and cardiovascular disease, Pharmacol. Ther. 143 (2014) 12–23.
[6] S.K. Byeon, J.Y. Lee, J.S. Lee, M.H. Moon, Lipidomic profiling of plasma and urine from patients with Gaucher disease during enzyme replacement therapy by nanoflow liquid chromatography–tandem mass spectrometry, J. Chromatogr. A 1381 (2015) 132–139.
[7] H.A. Brown, R.C. Murphy, Working towards an exegesis for lipids in biology, Nat. Chem. Biol. 5 (2009) 602–606.
[8] D.M. Lovinger, Communication networks in the brain, Alcohol Res. Health 31 (2008) 196–214.
[9] P. Scheiffele, Cell-cell signaling during synapse formation in the CNS, Annu. Rev. Neurosci. 26 (2003) 485–508.
[10] M. Miller, D. Speert, T. Bentsen, M. Fenichel, C. Fenichel, Brain Facts: A Primer on the Brain and Nervous System, 7th ed., Society for Neuroscience, Washington DC, USA, 2012.
[11] J.J. Palop, J. Chin, L. Mucke, A network dysfunction perspective on neurodegenerative diseases, Nature 443 (2006) 768–773.
[12] R.S. Yadav, N.K. Tiwari, Lipid integration in neurodegeneration: an overview of Alzheimer's disease, Mol. Neurobiol. 50 (2014) 168–176.
[13] X. Han, D.M. Holtzman, D.W. McKeel, J. Kelley, J.C. Morris, Substantial sulfatide deficiency and ceramide elevation in very early Alzheimer's disease: potential role in disease pathogenesis, J. Neurochem. 82 (2002) 809–818.
[14] H. Satoi, H. Tomimoto, R. Ohtani, T. Kitano, T. Kondo, M. Watanabe, et al., Astroglial expression of ceramide in Alzheimer's disease brains: a role during neuronal apoptosis, Neuroscience 130 (2005) 657–666.
[15] G. Poli, J.R. Schaur, 4-Hydroxynonenal in the pathomechanisms of oxidative stress, IUBMB Life 50 (2000) 315–321.
[16] L.M. Sayre, D.A. Zelasko, P.L. Harris, G. Perry, R.G. Salomon, M.A. Smith, 4-Hydroxynonenal-derived advanced lipid peroxidation end products are increased in Alzheimer's disease, J. Neurochem. 68 (1997) 2092–2097.
[17] C.P. Müller, M. Reichel, C. Mühle, C. Rhein, E. Gulbins, J. Kornhuber, Brain membrane lipids in major depression and anxiety disorders, Biochim. Biophys. Acta Mol. Cell Biol. Lipids 1851 (2015) 1052–1065.
[18] R.M. Adibhatla, J.F. Hatcher, Altered lipid metabolism in brain injury and disorders, Subcell. Biochem. 49 (2008) 241–268.
[19] C. Hu, H. Kong, F. Qu, Y. Li, Z. Yu, P. Gao, et al., Application of plasma lipidomics in studying the response of patients with essential hypertension to antihypertensive drug therapy, Mol. BioSyst. 7 (2011) 3271–3279.
[20] D.A. Brown, E. London, Functions of lipid rafts in biological membranes, Annu. Rev. Cell Dev. Biol. 14 (1998) 111–136.
[21] D.J. Selkoe, Alzheimer's disease: a central role for amyloid, J. Neuropathol. Exp. Neurol. 53 (1994) 438–447.
[22] A.P. Simopoulos, Human requirement for N-3 polyunsaturated fatty acids, Poult. Sci. 79 (2000) 961–970.
[23] R.P. Bazinet, S. Layé, Polyunsaturated fatty acids and their metabolites in brain function and disease, Nat. Rev. Neurosci. 15 (2014) 771–785.
[24] H.Y. Kim, M. Akbar, A. Lau, L. Edsall, Inhibition of neuronal apoptosis by docosahexaenoic acid (22: 6n-3) role of phosphatidylserine in antiapoptotic effect, J. Biol. Chem. 275 (2000) 35215–35223.
[25] F. Calderon, H.Y. Kim, Docosahexaenoic acid promotes neurite growth in hippocampal neurons, J. Neurochem. 90 (2004) 979–988.
[26] J.R. Hibbeln, Depression, suicide and deficiencies of omega–3 essential fatty acids in modern diets, World Rev. Nutr. Diet. 99 (2009) 17–30.
[27] M.C. Morris, The role of nutrition in Alzheimer's disease: epidemiological evidence,

Eur. J. Neurol. 16 (2009) 1–7.
[28] H.R. Park, M. Park, J. Choi, K.Y. Park, H.Y. Chung, J. Lee, A high-fat diet impairs neurogenesis: involvement of lipid peroxidation and brain-derived neurotrophic factor, Neurosci. Lett. 482 (2010) 235–239.
[29] S. Dutheil, K.T. Ota, E.S. Wohleb, K. Rasmussen, R.S. Duman, High-fat diet induced anxiety and anhedonia: impact on brain homeostasis and inflammation, Neuropsychopharmacology 41 (2016) 1874–1887.
[30] F.N. Jacka, N. Cherbuin, K.J. Anstey, P. Sachdev, P. Butterworth, Western diet is associated with a smaller hippocampus: a longitudinal investigation, BMC Med. 13 (2015) 215.
[31] M. Portovedo, L.M. Ignacio-Souza, B. Bombassaro, A. Coope, A. Reginato, D.S. Razolli, et al., Saturated fatty acids modulate autophagy's proteins in the hypothalamus, PLoS One 10 (2015) e0119850.
[32] C. Giles, R. Takechi, N.A. Mellett, P.J. Meikle, S. Dhaliwal, J.C. Mamo, The effects of long-term saturated fat enriched diets on the brain lipidome, PLoS One 11 (2016) e0166964.
[33] M.L. Borg, S.F. Omran, J. Weir, P.J. Meikle, M.J. Watt, Consumption of a high-fat diet, but not regular endurance exercise training, regulates hypothalamic lipid accumulation in mice, J. Physiol. 590 (2012) 4377–4389.
[34] R. Taguchi, J. Hayakawa, Y. Takeuchi, M. Ishida, Two-dimensional analysis of phospholipids by capillary liquid chromatography/electrospray ionization mass spectrometry, J. Mass Spectrom. 35 (2000) 953–966.
[35] G. Isaac, D. Bylund, J.E. Månsson, K.E. Markides, J. Bergquist, Analysis of phosphatidylcholine and sphingomyelin molecular species from brain extracts using capillary liquid chromatography electrospray ionization mass spectrometry, J. Neurosci. Methods 128 (2003) 111–119.
[36] Z. Zhao, Y. Xiao, P. Elson, H. Tan, S.J. Plummer, M. Berk, et al., Plasma lysophosphatidylcholine levels: potential biomarkers for colorectal cancer, J. Clin. Oncol. 25 (2007) 2696–2701.
[37] H.K. Min, G. Kong, M.H. Moon, Quantitative analysis of urinary phospholipids found in patients with breast cancer by nanoflow liquid chromatography–tandem mass spectrometry: II. Negative ion mode analysis of four phospholipid classes, Anal. Bioanal. Chem. 396 (2010) 1273–1280.
[38] D.Y. Bang, M.H. Moon, On-line two-dimensional capillary strong anion exchange/reversed phase liquid chromatography–tandem mass spectrometry for comprehensive lipid analysis, J. Chromatogr. A 1310 (2013) 82–90.
[39] M.H. Moon, Phospholipid analysis by nanoflow liquid chromatography-tandem mass spectrometry, Mass Spectrom. Lett. 5 (2014) 1–11.
[40] S.K. Byeon, J.C. Lee, B.C. Chung, H.S. Seo, M.H. Moon, High-throughput and rapid quantification of lipids by nanoflow UPLC-ESI-MS/MS: application to the hepatic lipids of rabbits with nonalcoholic fatty liver disease, Anal. Bioanal. Chem. 408 (2016) 4975–4985.
[41] J.C. Lee, I.Y. Kim, Y. Son, S.K. Byeon, D.H. Yoon, J.S. Son, et al., Evaluation of treadmill exercise effect on muscular lipid profiles of diabetic fatty rats by nanoflow liquid chromatography-tandem mass spectrometry, Sci. Rep. 6 (2016) 29617.
[42] S.M. Park, S.K. Byeon, H. Sung, S.Y. Cho, J.K. Seong, M.H. Moon, Lipidomic perturbations in lung, kidney, and liver tissues of p53 knockout mice analyzed by nanoflow UPLC-ESI-MS/MS, J. Proteome Res. 15 (2016) 3763–3772.
[43] S.T. Lee, J.C. Lee, J.W. Kim, S.Y. Cho, J.K. Seong, M.H. Moon, Global changes in lipid profiles of mouse cortex, hippocampus, and hypothalamus upon p53 knockout, Sci. Rep. 6 (2016) 36510.
[44] J.S. Yang, J.C. Lee, S.K. Byeon, K.H. Rha, M.H. Moon, Size dependent lipidomic analysis of urinary exosomes from patients with prostate cancer by flow field-flow fractionation and nanoflow liquid chromatography-tandem mass spectrometry, Anal. Chem. 59 (2017) 2488–2496.
[45] L. Ding, Z. Qu, J. Chi, R. Shi, L. Wang, L. Hou, et al., Effects of preventative application of metformin on bile acid metabolism in high fat-fed/streptozotocin-diabetic rats, Int. J. Clin. Exp. Pathol. 8 (2015) 5450.
[46] S.K. Byeon, J.Y. Lee, M.H. Moon, Optimized extraction of phospholipids and lysophospholipids for nanoflow liquid chromatography-electrospray ionization-tandem mass spectrometry, Analyst 137 (2012) 451–458.
[47] S. Lim, S.K. Byeon, J.Y. Lee, M.H. Moon, Computational approach to structural identification of phospholipids using raw mass spectra from nanoflow liquid chromatography–electrospray ionization–tandem mass spectrometry, J. Mass Spectrom. 47 (2012) 1004–1014.
[48] E.J. Ahn, H. Kim, B.C. Chung, G. Kong, M.H. Moon, Quantitative profiling of phosphatidylcholine and phosphatidylethanolamine in a steatosis/fibrosis model of rat liver by nanoflow liquid chromatography/tandem mass spectrometry, J. Chromatogr. A 1194 (2008) 96–102.
[49] S.M. Park, S.K. Byeon, H. Lee, H. Sung, I.Y. Kim, J.K. Seong, et al., Lipidomic analysis of skeletal muscle tissues of p53 knockout mice by nUPLC-ESI-MS/MS, Sci. Rep. 7 (2017) 3302.
[50] J. Kopecký, K. Flachs, P. Bardová, T. Brauner, J. ŠponarovÁ PražÁk, Modulation of lipid metabolism by energy status of adipocytes, Ann. N. Y. Acad. Sci. 967 (2002) 88–101.
[51] D.M. Erion, G.I. Shulman, Diacylglycerol-mediated insulin resistance, Nat. Med. 16 (2010) 400–402.
[52] S.E. Arnold, I. Lucki, B.R. Brookshire, G.C. Carlson, C.A. Browne, H. Kazi, et al., High-fat diet produces brain insulin resistance, synaptodendritic abnormalities and altered behavior in mice, Neurobiol. Dis. 67 (2014) 79–87.
[53] H. Blasco, C. Veyrat-Durebex, C. Bocca, F. Patin, P. Vourc'h, J.K. Nzoughet, G. Lenaers, C.R. Andres, G. Simard, P. Corcia, P. Reynier, Lipidomics reveals cerebrospinal-fluid signatures of ALS, Sci. Rep. 15 (2017) 17652.
[54] K. Bozek, Y. Wei, Z. Yan, X. Liu, J. Xiong, M. Sugimoto, et al., Organization and evolution of brain lipidome revealed by large-scale analysis of human, chimpanzee, macaque, and mouse tissues, Neuron 85 (2015) 695–702.
[55] G. Cermenati, N. Mitro, M. Audano, R.C. Melcangi, M. Crestani, E. De Fabiani, et al., Lipids in the nervous system: from biochemistry and molecular biology to pathophysiology, Biochim. Biophys. Acta Mol. Cell Biol. Lipids 1851 (2015) 51–60.
[56] E. Lauwers, R. Goodchild, P. Verstreken, Membrane lipids in presynaptic function and disease, Neuron 90 (2016) 11–25.
[57] A. Schwarz, E. Rapaport, K. Hirschberg, A.H. Futerman, A regulatory role for sphingolipids in neuronal growth inhibition of sphingolipid synthesis and degradation have opposite effects on axonal branching, J. Biol. Chem. 270 (1995) 10990–10998.
[58] J. Zhang, Q. Liu, Cholesterol metabolism and homeostasis in the brain, Protein Cell 6 (2015) 254–264.
[59] S.C. Frasch, D.L. Bratton, Emerging roles for lysophosphatidylserine in resolution of inflammation, Prog. Lipid Res. 51 (2012) 199–207.
[60] C.N. Ochner, D.M. Barrios, C.D. Lee, F.X. Pi-Sunyer, Biological mechanisms that promote weight regain following weight loss in obese humans, Physiol. Behav. 120 (2013) 106–113.
[61] J.A. Luchsinger, M.X. Tang, S. Shea, R. Mayeux, Caloric intake and the risk of Alzheimer disease, Arch. Neurol. 59 (2002) 1258–1263.
[62] S. Craft, The role of metabolic disorders in Alzheimer disease and vascular dementia: two roads converged, Arch. Neurol. 66 (2009) 300–305.
[63] L.R. Freeman1, V. Haley-Zitlin, D.S. Rosenberger, A.-C. Granholm, Damaging effects of a high-fat diet to the brain and cognition: a review of proposed mechanisms, Nutr. Neurosci. 17 (2014) 241–251.
[64] O. Guillemot-Legris, G.G. Muccioli, Obesity-induced neuroinflammation: beyond the hypothalamus, Trends Neurosci. 40 (2017) 237–253.
[65] R. Takechi, N.M. Pallebage-Gamarallage, V. Lam, C. Giles, J.C. Mamo, Nutraceutical agents with anti-inflammatory properties prevent dietary saturated-fat induced disturbances in blood–brain barrier function in wild-type mice, J. Neuroinflammation 10 (2013) 73–84.
[66] M.S. Spagnuolo, M.P. Mollica, B. Maresca, G. Cavaliere, C. Cefaliello, G. Trinchese, R. Scudiero, M. Crispino, L. Cigliano, High fat diet and inflammation – modulation of haptoglobin level in rat brain, Front. Cell. Neurosci. 9 (2015) 479–491.